Available online at www.sciencedirect.com
SCIENCE DIRECT®
Journal of Nuclear Materials 334 (2004) 9–12
journal of nuclear materials
www.elsevier.com/locate/jnucmat

# Channelling studies on the lattice location of B atoms in graphite

Eiichi Yagi [a,b,*], Tadao Iwata [c,1], Teruo Urai [a], Kiyoshi Ogiwara [a]

[a] RIKEN (The Institute of Physical and Chemical Research), Wako, Saitama 351-0198, Japan
[b] The School of Science and Engineering, Waseda University, 3-4-1 Ohkubo, Shinjuku-ku, Tokyo 162-8601, Japan
[c] Japan Atomic Energy Research Institute, Tokai-mura, Naka-gun, Ibaraki-ken 319-1195, Japan

Received 2 November 2003; accepted 12 April 2004

**Abstract**

In order to obtain information on the lattice location of B atoms in graphite, channelling experiments have been performed at room temperature with a proton beam of an energy of 0.65–0.77 MeV for the ⟨0 0 0 1⟩ axial channel in highly oriented pyrolytic graphite (HOPG) crystals doped with 0.32 at.% B. The B atoms are detected by measuring α-particles which are emitted as a result of a nuclear reaction $^{11}B(p,\alpha)\alpha\alpha$. It is clearly demonstrated that most of B atoms are shadowed behind the ⟨0 0 0 1⟩ C atomic rows. Taking account of the already reported experimental results on a change of lattice parameters by B-doping, it is concluded that most of B atoms are located at substitutional sites. It is also observed that B-doping introduces lattice strain on the *c*-plane. In addition, the presence of a small portion of interstitial B atoms is suggested.


*PACS:* 62.72.−y; 61.72.Ji; 61.72.Dd

## 1. Introduction

Boron has a favourable effect on graphitization of carbon. A number of properties of graphite are influenced by the presence of boron in the lattice. The boron atom is expected to act as an acceptor, when it substitutes a carbon atom, because it has one less valence electron than carbon. Regarding where boron atoms are located in a graphite crystal lattice, experimental results on the B concentration dependence of lattice parameters [1,2], density [1], and electronic properties [3,4] suggest that boron occupies a substitutional site, replacing a carbon atom. In the present study, in order to obtain additional direct information on the lattice location of boron atoms, channelling experiments are performed on B-doped graphite crystals. There exist ⟨0 0 0 1⟩ axial channels surrounded by C atomic rows in the *c*-direction and also {0 0 0 1} planar channels between *c*-planes in perpendicular to the *c*-direction. It has been demonstrated for undoped graphite crystals that channelling experiment is possible for the ⟨0 0 0 1⟩ channel [5,6]. Fig. 1 shows the crystal structure of graphite, where an open channel along the *c*-axis (the ⟨0 0 0 1⟩ channel) is indicated by broken lines. This channel is surrounded by two kinds of C atomic rows; one with the interatomic distance equal to the interlayer spacing $c_0$ and another with that of $2c_0$.

## 2. Experimental

Specimens are highly oriented pyrolytic graphite (HOPG) crystals and those doped with 0.32 at.% B

* Corresponding author. Address: RIKEN, Wako, Saitama 351-0198, Japan. Tel.: +81-48 467 9385; fax: +81-48 462 4645.
*E-mail address:* eyagi@postman.riken.go.jp (E. Yagi).
[1] Present address: 1883-1 Toyooka, Tokai-mura, Ibaraki-ken 319-1105, Japan.

0022-3115/$ - see front matter © 2004 Elsevier B.V. All rights reserved.
doi:10.1016/j.jnucmat.2004.04.321

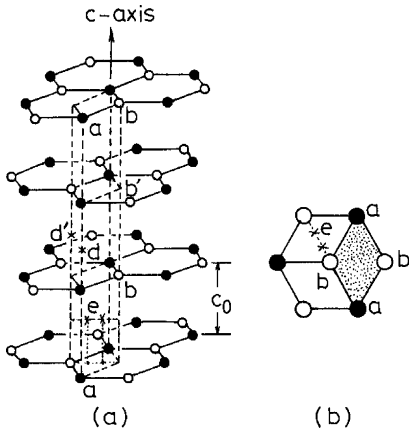


Fig. 1. (a) The crystal structure of graphite. A $\langle 0\,0\,0\,1\rangle$ channel is indicated by broken lines. It is surrounded by two types of C atomic rows, *aa* and *bb*. (b) The projection of the $\langle 0\,0\,0\,1\rangle$ channel onto the plane perpendicular to the *c*-axis.

supplied from Union Carbide Corporation (two doped specimens taken from different bulk crystals; specimen-1 and specimen-2). B atoms were detected utilizing a nuclear reaction $^{11}B(p,\alpha)\alpha\alpha$ with a proton beam [7,8]. This reaction exhibits a broad resonance at proton energies around 0.62 MeV. The reaction cross section reaches maximum (~90 mb/sr) at 0.624 MeV and the resonance width (FWHM) is about 0.3 MeV [9]. As a result of the reaction α-particles are emitted. In the present experiments this resonance reaction is utilized for the detection of B atoms; the B atoms are detected by measuring the α-particles, whose energy extends up to about 5 MeV.

Channelling experiments were performed at room temperature with a 0.65–0.77 MeV proton beam for the $\langle 0\,0\,0\,1\rangle$ axial channel. The beam was collimated to have divergence less than 0.076°. The beam size was 1 mm in diameter and the beam intensity was 1–2 nA. The specimen was mounted on the specimen holder of the three-axis goniometer. Backscattered protons and emitted α-particles were measured at angles of 160° and 150°, respectively, as a function of the incident angle with respect to the *c*-axis in a similar way as described in Ref. [10]. In the case of measurements of α-particles, Mylar foil or Al foil was placed in front of the detector as an energy absorber. Channelling measurement for the $\{0\,0\,0\,1\}$ planar channel was also tried, but it was unsuccessful, due probably to difficulties in preparation of surface suitable for channelling experiments and also due to a shallow dip. For this planar channelling experiments, surface treatment was carried out by sputtering with a 5 keV Ar beam in an oblique direction to the surface, but it was unsuccessful, because Ar ions were observed to be implanted in the surface layer.

## 3. Results and discussion

Fig. 2 shows the channelling angular profiles obtained for the undoped specimen and the B-doped specimen-2 with a 0.768 MeV proton beam for the protons backscattered by C atoms at a depth of 0.25 μm from the surface. They exhibit a simple dip (C-dip). The C-dip for the B-doped specimen is shallower and broader than that for the undoped specimen, indicating the deterioration of the crystallinity. Fig. 3 shows the dependence of the minimum yield ($\chi_{min}$) in the C-dip on the depth where the protons are scattered by C atoms. This dependence is used as a measure of dechannelling. The $\chi_{min}$ is larger and depends more weakly on the depth in the B-doped specimen than in the undoped specimen.

Fig. 4 shows the angular profiles of backscattered protons (C-profile) and α-particles (B-profile) measured for two different B-doped specimens (the specimen-1

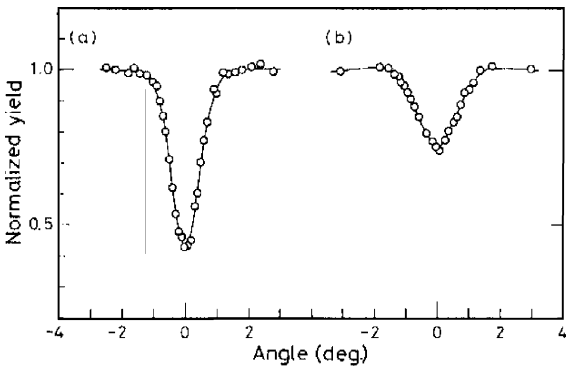


Fig. 2. The channelling angular profiles obtained for (a) the undoped specimen and (b) the B-doped specimen-2 with a 0.768 MeV proton beam for the protons backscattered by C atoms at a depth of 0.25 μm from the surface.

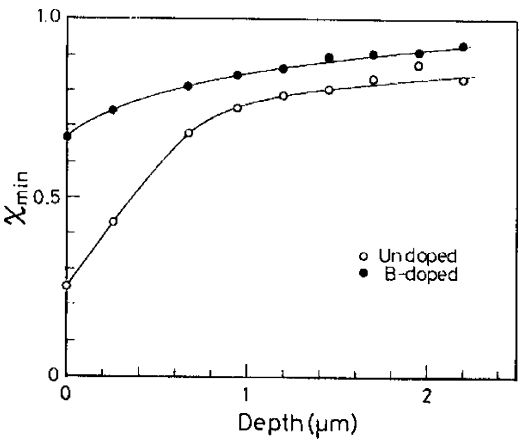


Fig. 3. The dependence of the minimum yield ($\chi_{min}$) in the C-dip in Fig. 2 on the depth where the protons are scattered by C atoms.

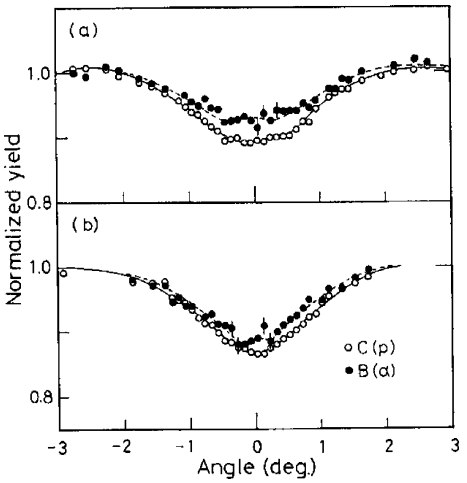


Fig. 4. The channelling angular profiles of backscattered protons and emitted α-particles obtained with a 0.768 MeV proton beam at room temperature for (a) the B-doped specimen-1 and (b) the B-doped specimen-2. The α-particles were measured with an energy absorber of 4 μm Mylar foil. The depth region chosen to obtain the angular profile is described in the text; from surface to 2.8 μm for C-profile, and from surface to deeper than 3.3 μm for B-profile. The full curves and the broken curves were drawn only to guide the eye.

and -2) with a 0.768 MeV proton beam with an energy absorber of 4 μm thick Mylar foil in front of the α-particle detector. Both profiles exhibit shallow dips with approximately the same angular half width, but the B-dip is shallower than the C-dip. Although the statistical error is not small, in the B-profile there seems to be a small central peak being superimposed on the shallow dip, suggesting the presence of a small portion of interstitial B atoms. The C- and B-profiles in Fig. 4 were obtained for the total yield in the whole region of the energy spectrum of the backscattered protons and that of α-particles, respectively. These energy regions correspond to different depth regions as described below. By the RBS (Rutherford backscattering spectroscopy) method with the 0.768 MeV proton beam, the depth region deeper than about 2.8 μm from the surface cannot be probed. On the other hand, the energy spectrum of α-particles includes α-particles emitted from a region deeper than 2.8 μm. At a depth of 3.3 μm from the surface, the energy of protons decreases to 0.475 MeV, where the nuclear reaction cross section is still a half of the maximum value at the resonance, and the high energy α-particles emitted there can be detected after penetrating the 4 μm thick Mylar foil. Therefore, due to the increasing dechannelling effect of the proton beam in a deeper region (Fig. 3), the observed B-dip is shallower than the dip which could be obtained for the α-particles emitted from the same depth region as probed by the RBS spectrum, i.e., within the depth region from surface

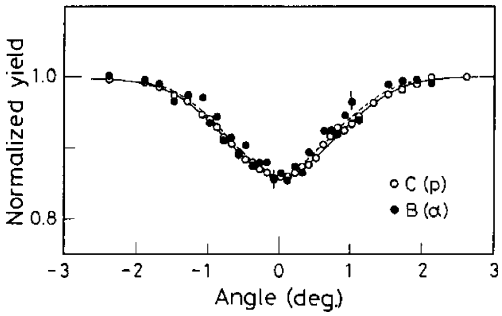


Fig. 5. The channelling angular profiles of backscattered protons and emitted α-particles obtained with a 0.666 MeV proton beam at room temperature for the B-doped specimen-2. The α-particles were measured with an energy absorber of 13 μm Al foil. The depth region chosen to obtain the angular profiles is described in the text; from surface to 1.75 μm. The full curve and the broken curve were drawn only to guide the eye.

to 2.8 μm. In order to compare the C-and B-angular profiles for approximately the same depth region, Al foil 13 μm thick was placed in front of the α-particle detector. Fig. 5 shows the angular profiles thus measured with a 0.666 MeV proton beam for the specimen-2, but at a different spot from that where Fig. 4 was measured. The 13 μm thick Al foil discriminates most of α-particles which were emitted from the region deeper than 1.75 μm from the surface. Correspondingly, the C-angular profile was obtained for the protons backscattered by C atoms within approximately the same depth region from the surface to 1.75 μm. Both angular profiles exhibit the dips with the same angular half-width (FWHM) of 1.8° and the same $\chi_{min}$ of 0.86 within the experimental accuracy. Taking account of this result, it is considered that the difference in the depth of the channelling dip between C- and B-angular profiles in Fig. 4 is due mainly to the difference in the depth region which was chosen to obtain each angular profile. From Figs. 4 and 5 it is demonstrated that most of B atoms are shadowed behind the $\langle 0\,0\,0\,1\rangle$ C atomic rows, and that a small portion of B atoms might be located at interstitial sites, which are projected around the centre of the $\langle 0\,0\,0\,1\rangle$ channel, in the specimen-1 and also, depending on the spot examined, in the specimen-2.

As the sites shadowed behind the $\langle 0\,0\,0\,1\rangle$ C atomic rows, there are three types of sites; (1) a substitutional site, (2) a centre of a hexagon (a $b'$-site in Fig. 1) and (3) any site between two $c$-planes on the $\langle 0\,0\,0\,1\rangle$ atomic row ($d$- and $d'$-sites in Fig. 1). The first two types of sites are on the $c$-plane. The latter two sites ($d$- and $d'$-sites) are interstitial sites. As the measurement for the $\{0\,0\,0\,1\}$ planar channel was unsuccessful, it is impossible to make distinction between the first two types of sites and the latter two sites. It is widely accepted that the $d'$-site is stable, whereas the $b'$- and $d$-sites are unstable because of a large repulsive force from adjacent atoms [11]. On

the other hand, Taji et al. calculated the configuration of an interstitial C atom by the molecular dynamical method and found that the stable site for the interstitial C atom is not the $d'$-site on the $b$-atomic row, but a site displaced by 0.26–0.39 Å from the $d'$-site toward the channel centre between two $c$-planes, i.e., the $e$-site in Fig. 1 [12]. The magnitude of the displacement varies depending on the relative position of the interstitial atom to the boundaries of the model crystal used in the calculation. If the B atoms are located either at the $d'$-site or at the $e$-site, the $c$-spacing should increase with increasing B concentration. However, the results of the X-ray diffraction experiments show that the $c$-spacing decreases with B concentration [1,2]. Hence, it is concluded that most of B atoms are not located at interstitial sites, but at substitutional sites.

The presence of a small portion of interstitial B atoms around the centre of the $\langle 0\,0\,0\,1\rangle$ channel is suggested in Fig. 4. The present experimental result cannot refer to whether this kind of interstitial site is located on the $c$-plane or between $c$-planes. The existence of interstitial B atoms has also been suggested. Turnbull et al. explained their experimental results on the change of lattice parameters during heat treatment of as-prepared B-doped graphite crystals by supposing the existence of both interstitial and substitutional B atoms [13]. Studies on the effect of B on the electronic properties of graphite indicate that B-doping introduces holes, but its efficiency is less than 100%, i.e., less than that expected for the perfect substitution of B atoms [3]. This might be related partly to the presence of the interstitial B atoms.

Considering that most of B atoms are located at substitutional sites, the increase of $\chi_{min}$ of C-dip on B-doping (Figs. 2 and 3) is attributed to the distortion of the $c$-plane in the graphite lattice; B-doping induces lattice strain on the $c$-plane. This is consistent with the investigation by the Raman scattering method, in which a new band at 1360 $cm^{-1}$ characteristic in ground graphite or irradiated graphite became observed on B-doping [14,15]. The result of the Raman scattering was interpreted to be that the B-doping introduced a local distortion around substitutional B atoms on the $c$-planes.

## 4. Summary

The lattice location of B atoms doped with 0.32 at.% in graphite was investigated at room temperature by the channelling method utilizing a nuclear reaction $^{11}B(p,\alpha)\alpha\alpha$ with a proton beam of an energy of 0.65–0.77 MeV. It was clearly observed that most of B atoms are shadowed behind the $\langle 0\,0\,0\,1\rangle$ C atomic rows. Taking account of the published results on a change of lattice parameters by B-doping, it was concluded that most of B atoms are located at substitutional sites. In addition, the presence of a small portion of interstitial B atoms was suggested.

## Acknowledgements

One of the authors (E.Y.) would like to thank Dr Y. Yano for his support in various phases in performing this research. The authors thank Dr A. Nakao for her help in a trial of sputtering with an Ar beam for surface treatment.

## References

[1] C.E. Lowell, J. Am. Ceram. Soc. 50 (1967) 142.
[2] P. Wagner, J.M. Dickinson, Carbon 8 (1970) 313.
[3] D.E. Soule, in: Proceedings of Vth Conference on Carbon, vol. 1, Pergamon Press, New York, 1962, p. 13.
[4] S. Marinkovic, in: P.A. Thrower (Ed.), Chemistry and Physics of Carbon, vol. 19, Marcel Dekker, New York, 1984, p. 1.
[5] T. Iwata, K. Komaki, H. Tomimitsu, K. Kawatsura, K. Ozawa, K. Doi, Radiat. Eff. 24 (1975) 63.
[6] B.S. Elman, G. Braunstein, M.S. Dresselhaus, G. Dresselhaus, T. Venkatesan, B. Wilkens, J. Appl. Phys. 56 (1984) 2114.
[7] V.D. Dehnhard, D. Kamke, P. Kramer, Ann. Phys. (Germany) 14 (1964) 201.
[8] O. Beckman, T. Huus, C. Zupancic, Phys. Rev. 91 (1953) 606.
[9] E. Ligeon, A. Bontemps, J. Radioanal. Chem. 12 (1972) 335.
[10] K. Tanaka, E. Yagi, N. Masahashi, Y. Mizuhara, K. Tatsumi, T. Takahari, Nucl. Instrum. and Meth. B 45 (1990) 471.
[11] B.T. Kelly, Physics of Graphite, Applied Science, London, 1981.
[12] Y. Taji, T. Yokota, T. Iwata, J. Phys. Soc. Jpn. 55 (1986) 2676.
[13] J.A. Turnbull, M.S. Stagg, W.T. Eeles, Carbon 3 (1966) 387.
[14] T. Hagio, M. Nakamizo, K. Kobayashi, Carbon 25 (1987) 637.
[15] T. Hagio, M. Nakamizo, K. Kobayashi, Carbon 27 (1989) 259.